Published on 17 November 2009. Downloaded by Universitat Autonoma de Barcelona on 27/10/2014 09:31:36.

This paper is published as part of a *Dalton Transactions* themed issue on:

Metal Anticancer Compounds

Guest Editor Peter Sadler

University of Warwick, UK

Published in issue 48, 2009 of *Dalton Transactions*

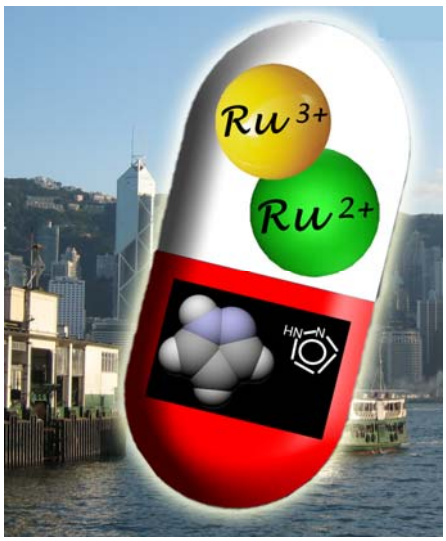

Image reproduced with permission of Chi-Ming Che

Articles published in this issue include:

PERSPECTIVES:

Non-traditional platinum compounds for improved accumulation, oral bioavailability, and tumor targeting
Katherine S. Lovejoy and Stephen J. Lippard, *Dalton Trans.,* 2009, DOI**:** 10.1039/b913896j

Metal complexes as photochemical nitric oxide precursors: Potential applications in the treatment of tumors
Alexis D. Ostrowski and Peter C. Ford, *Dalton Trans.,* 2009, DOI: 10.1039/b912898k

Novel and emerging approaches for the delivery of metallo-drugs
Carlos Sanchez-Cano and Michael J. Hannon, *Dalton Trans.,* 2009, DOI: 10.1039/b912708a

HOT ARTICLE:

Iron(III) complexes of fluorescent hydroxamate ligands: preparation, properties, and cellular processing
Antonia J. Clarke, Natsuho Yamamoto, Paul Jensen and Trevor W. Hambley**,** *Dalton Trans.,* 2009, DOI**:** 10.1039/b914368h

Visit the *Dalton Transactions* website for more cutting-edge inorganic and bioinorganic research
www.rsc.org/dalton

Published on 17 November 2009. Downloaded by Universitat Autonoma de Barcelona on 27/10/2014 09:31:36.

Reactions of palladium and gold complexes with zinc-thiolate chelates using electrospray mass spectrometry and X-ray diffraction: molecular identification of [Pd(bme-dach)], $[Au(bme\text{-}dach)]^+$ and $[ZnCl(bme\text{-}dach)]_2Pd$†

Queite A. de Paula,[a] Qin Liu,[a] Elky Almaraz,[b] Jason A. Denny,[b] John B. Mangrum,[a] Nattamai Bhuvanesh,[b] Marcetta Y. Darensbourg[b] and Nicholas P. Farrell*[a]

Received 27th August 2009, Accepted 10th November 2009
First published as an Advance Article on the web 17th November 2009
DOI: 10.1039/b917748p

The reaction between the complexes $[MCl(L)]Cl_x$ (L = 2,2′,2″-terpyridine, terpy and dien, diethylenetriamine; M = Pd, $x = 1$; M = Au, $x = 2$) and $[Zn(bme\text{-}dach)]_2$, an N_2S_2-Zn-thiolate bridged dimer used to mimic zinc finger protein sites, was studied by Electrospray Ionisation Mass Spectrometry and the structures of some of the products confirmed by X-ray crystallography. All reactions investigated in this work gave heteronuclear (Zn-thiolate)-metal products, the predominant species being the trinuclear dithiolate-bridged aggregate $\{[Zn(bme\text{-}dach)]_2M\}^{n+}$ (M = Pd, Au). X-Ray diffraction studies verified the molecular structure of $[\{ZnCl(bme\text{-}dach)\}_2Pd]$, and further confirmed that the zinc within the $[Zn(bme\text{-}dach)]_2$ unit was retained within the N_2S_2 binding site. The Zn-bound thiolates form stable thiolate bridges to Pd^{2+} in a stair-step shape, held together by a planar PdS_4 center. In addition, both zinc atoms maintained penta-coordinate coordination with apical chloride ligands rather than the more commonly observed tetrahedral geometry. Further, [Pd(bme-dach)] was directly synthesized for X-ray structural characterization of the metal exchanged product observed in mass spectrometry experiments. In the case of Au compounds, the reactions were very fast and the products were similar for both $[AuCl(L)]Cl_2$ (L = terpy and dien) starting materials. In addition to the multimetallic Zn,Au,Zn aggregate formation, the predominant species from the reaction between $[Zn(bme\text{-}dach)]_2$ and both Au compounds was the $[Au(bme\text{-}dach)]^+$ cation observable *via* ESI-MS, suggesting Zn/Au metal exchange immediately after mixing the compounds. The direct synthesis of $[Au(bme\text{-}dach)]BPh_4$ confirmed the molecular structure of this species through X-ray crystallography. The reactivity profile of Pd^{2+} and Au^{3+} species is compared with previous studies using the isostructural Pt compounds and the biological relevance of the results discussed.

Introduction

Zinc finger (ZF) proteins are the most frequently used class of transcription factors, accounting for 3% of genes in the human genome.[1,2] These structural elements are associated with protein-nucleic acid and protein-protein interactions. They display many diverse functions, including DNA recognition, RNA packaging, protein folding and assembly, transcriptional activation as well as cell differentiation and growth.[3,4] The most common ligands for Zn^{2+} in zinc finger proteins are cysteine (S donor) and histidine (N donor) in Cys_2His_2, Cys_3His and Cys_4 coordination motifs. The Cys residues of Zn^{2+} are reactive and changes in the cellular redox state and/or exposure to electrophilic agents can alter DNA binding activities of ZF transcription factors.[5] Several metals, including Cd^{2+}, Hg^{2+}, Pb^{2+}, Ni^{2+}, Pt^{2+}, Co^{2+}, and Fe^{2+} have been shown to substitute Zn^{2+} in zinc finger domains.[6,7]

Inactivation of zinc fingers may also be a mechanism of action for metallodrugs. Specifically, platinum-nucleobase compounds such as *trans*-$[PtCl(9\text{-}EtGua)(pyr)_2]^+$ and *SP-4-2*-$[PtCl(9\text{-}EtGua)(NH_3)(quinoline)]^+$ have moderate antiviral selectivity and can form ternary adducts with the C-terminal finger of HIV NCp7 (*F2*) with eventual ejection of Zn^{2+} and incorporation of Pt^{2+} into the binding site.[8,9] Zinc-Finger-Pt-DNA interactions may also be relevant for those proteins which recognize platinated DNA (Sp1, UVrABC).[10] The anti-arthritic gold compound, aurothiomalate, diminishes OB2-1 dependent c-erbB-2 transcription by inhibiting the binding of this positively acting transcription factor to DNA.[11] The purported zinc site of OB2-1 was suggested as the target. More specifically, aurothiomalate interacts with the Cys_2His_2 zinc fingers of TFIIIA and Sp1 with subsequent inhibition of the DNA-binding activity of the protein.[5] Studies using a model peptide based on the third zinc finger of Sp1 confirmed that Au^{1+} binding triggered zinc release.[5] It has been found that the formation of Au^{1+} aqua complexes are often unstable and may disproportionate to form Au^0 and Au^{3+} species.[12] It has been suggested that certain side effects brought about during gold(I) anti-arthritic therapy are due

[a]*Department of Chemistry, Virginia Commonwealth University, Richmond, Virginia 23284-2006, USA. E-mail: npfarrell@vcu.edu; Fax: 804-828-8599; Tel: 804-828-6320*
[b]*Department of Chemistry, Texas A&M University, College Station, TX 77842, USA*

† Electronic supplementary information (ESI) available: Ball and stick images of the [Pd(bme-dach)] structural disorder, mass spectral data of Au^{3+} compounds with Zn compounds. CCDC reference numbers 743609–743611. For ESI and crystallographic data in CIF or other electronic format see DOI: 10.1039/b917748p

 This journal is © The Royal Society of Chemistry 2009

Published on 17 November 2009. Downloaded by Universitat Autonoma de Barcelona on 27/10/2014 09:31:36.

to the formation of Au^{3+} complexes. Further, evidence has been presented for Au^{3+} reduction followed by release of the bound ligand and eventual coordination of a Au^{1+} ion to a protein side chain when Au^{3+} anticancer compounds are allowed to react with ubiquitin and cytochrome c.[13] To explore Au^{3+} reactivity with the $[Zn(bme\text{-}dach)]_2$ model, the present work supports the possible products resulting from Zn^{2+}-S-Au^{3+} interactions. Additionally, antiparasitic antimony compounds also trigger zinc release in model zinc fingers, a potentially novel mechanism of action for these drugs.[14]

The details of metal and ligand displacement on biomolecules such as zinc fingers are thus of general interest. We have therefore begun a biomimetic project to understand the molecular mechanism of zinc ejection by platinum and platinum-metal compounds using small molecule models.[15,16] In this respect, we have drawn an analogy between alkylation and platination of biological substrates.[8,15] Thiolate-bridged penta-coordinate zinc chelates such as $[Zn(bme\text{-}dach)]_2$, a $Zn(N_2S_2)$ dimer, are models for zinc proteins and are functional in terms of their S-alkylation reactivity. S-methylation of zinc-tethered thiolates occurs in the closely related $[Zn(bme\text{-}daco)]_2$ complex and its Cd analog.[17] The electrophilic reactivity of a similar $Zn(N_2S_2)$ complex was explored by Grapperhaus *et al.*, where S-alkylation by MeI and S-oxygenation with H_2O_2 indicate the reactivity of zinc-bound thiolates.[18,19]

In reactions with representative monofunctional complexes [PtCl(dien)]Cl or [PtCl(terpy)]Cl with $[Zn(bme\text{-}dach)]_2$, monothiolate and dithiolate-bridged heteronuclear Zn-(μ-SR)-Pt species as well as trinuclear Zn-(μ-SR)$_2$-Pt-(μ-SR)$_2$-Zn aggregates were structurally characterized and the products are a result of initial platination of the zinc cysteinate.[16] The product of direct displacement of Zn, [Pt(bme-dach)], was also characterized. In the case of $[PtCl(terpy)]^+$, a novel ligand exchange occurred with formation of $[ZnCl(terpy)]^+$, whereas the [PtCl(dien)]Cl reaction did not yield the corresponding $[ZnCl(dien)]^+$ ion. Thus, the nature of the ligand (dien, terpy) on the Pt moiety dictates to some extent the reactivity pattern. Platination with the [Pt(dien)] and [Pt(terpy)] moieties further strengthens the analogy between alkylation and platination of the Zn-thiolate bond.

To check the generality of the chemistry described above between Pt complexes and Zn models, we have now examined the isostructural compounds of Pd^{2+} and Au^{3+}. This allows comparison of the effects of isostructural d^8 complexes that differ in substitution kinetics. In addition, ligand (pyridine) substitution reactions have been shown to be significantly faster for $[PtCl(terpy)]^+$ than for $[PtCl(dien)]^+$.[20] The propensity for π-stacking of the terpy ligand with other π systems allows for comparison of structural effects with the dien ligand.[21] It is further relevant that a square planar Pd^{2+} complex of bis(2-mercaptoethyl)-1,4-diazacyclooctane, [Pd(bme-daco)], has been characterized and probed for its thiolate reactivity with small molecules.[17,22,23] The daco derivative contains one more carbon atom in the diazacyclo backbone than the H_2bme-dach (bis(2-mercaptoethyl)-1,4-diazacycloheptane) ligand system which has been used in this study.[17,22] In this contribution, we report mass spectrometry (ESI-MS) studies of the reactions of Pd^{2+} and Au^{3+} compounds with the Zn-thiolate dimer, with complementary MS/MS data to indicate the structure of new species formed. X-ray crystallography of $\{[ZnCl(bme\text{-}dach)]_2Pd\}$ and the directly synthesized $[Au(bme\text{-}dach)]BPh_4$ and [Pd(bme-dach)] confirmed the proposed structures. The structural parameters of the latter species were further compared with isostructural analogs of Ni^{2+} and Pt^{2+}.

Experimental

Chemical synthesis and physical methods

The complexes $[Zn(bme\text{-}dach)]_2$,[16] [PdCl(terpy)]Cl,[24] [AuCl-(terpy)]Cl_2 and [AuCl(dien)]Cl_2 were prepared as described in the literature.[24,25] Elemental analysis (C,H,N) for each precursor corresponded to the expected calculated values. The ESI-MS spectra for each starting material is shown in Figures S1 and S2.†

Synthesis

Modified synthesis of chloro(diethylenetriamine)palladium chloride, [PdCl(dien)]Cl (1). This is a new method for the synthesis of this compound compared to that reported.[24] The salt K_2PdCl_4 (130 mg, 0.40 mmol) was dissolved in 5 mL of deionized H_2O and the solution was filtered to remove impurities. The diethylenetriamine (dien) ligand (43.5 μL, 0.04 mmol) was dissolved in 1.0 mL of H_2O and the resulting solution was heated to 30 °C. The Pd solution was added drop wise to the ligand solution while stirring. A yellow precipitate formed initially, which dissolved in the course of the subsequent drop-wise addition. The temperature of the reaction solution was increased slowly during a 3 h period and then maintained at 100 °C for 20 min. The resulting yellow solution was reduced *in vacuo* to a small volume and stored overnight at 2 °C. Yellow crystals were filtered off, washed with ether/chloroform, and vacuum-dried; yield 90%. ESI-Mass Spectrum in MeOH $[M]^+$ m/z = 244.87 ($[PdCl(dien)]^+$); Anal. Calcd. for $C_4H_{13}N_3Cl_2Pd_1$ (Mr = 280.49 g mol^{-1}): C, 17.13; H, 4.67; N, 14.98. Found: C, 17.20; H, 4.60; N, 14.87.

Synthesis of N,N′-bis(2-mercaptoethyl)-1,4-diazacycloheptane-zincchloropalladate, [{ZnCl(bme-dach)}$_2$Pd] (2). $[Zn(bme\text{-}dach)]_2$ (5.60 mg, 0.010 mmol) was partially dissolved in 10.0 mL of MeOH and the mixture was heated for 10 min at 90 °C. Upon slow addition of a methanolic solution of [PdCl(terpy)]Cl in either 1 : 1 or 2 : 1 Pd : Zn stoichiometry, a yellow solid appeared immediately. The yellow product has low solubility in CH_3CN and $CHCl_3$, but was completely soluble in DMSO. The crystals of the $[\{ZnCl(bme\text{-}dach)\}_2Pd]$ were obtained by layering of $CHCl_3$/ether solvents. Anal. Calcd. for $C_{18}H_{36}N_4Cl_2S_4Zn_2Pd_1$ (Mr = 744.90 g mol^{-1}): C, 29.02; H, 4.87; N, 7.52. Found: C, 29.47; H, 4.83; N, 7.24.

Direct synthesis of N,N′-bis(2-mercaptoethyl)-1,4-diazacycloheptane palladium(II), [Pd(bme-dach)] (3). Under an inert atmosphere, a solution of NaOMe (0.470 g, 0.870 mmol) in 10 mL of MeOH was added to H_2bme-dach (0.188 g, 0.853 mmol) in 15 mL of MeOH and allowed to stir for 1.5 h at 22 °C. The $PdCl_2$ (0.151 g, 0.852 mmol) was dissolved in a mixture of 7 mL deionized H_2O and 20 mL MeOH, and cannulated into the stirring ligand solution. After 2 d of stirring at 22 °C under an Ar blanket, a black precipitate was removed *via* filtration; the yellow filtrate was concentrated *in vacuo* and purified through silica column chromatography (5 cm × 25 cm) with MeOH as the eluent. The air-stable product was collected from the mobile pale yellow band and

Published on 17 November 2009. Downloaded by Universitat Autonoma de Barcelona on 27/10/2014 09:31:36.

dried *in vacuo* to yield 0.100 g (0.309 mmol, 36.2%) of [Pd(bme-dach)]. Large, needle-shaped X-ray quality crystals were acquired by slow N_2 flow over a MeOH solution of product. ESI-Mass Spectrum in MeOH: $[M + H^+]^+$ $m/z = 325$; Anal. Calcd. for $C_9H_{18}N_2S_2Pd_0H_2O$ (Mr = 342.80 g mol^{-1}): 31.58; H, 5.89; N, 8.19. Found: C, 31.98; H, 5.29; N, 7.57.

Direct synthesis of N,N′-bis(2-mercaptoethyl)-1,4-diazacycloheptane gold(III) tetraphenylborate, [Au(bme-dach)]BPh$_4$ (4). Under Ar, H_2bme-dach (0.096 g, 0.436 mmol) was dissolved in 15 mL MeOH, and KOH (0.050 g, 0.891 mmol) in 15 mL MeOH was slowly added. The solution was vigorously stirred for 1 h at 22 °C. $KAuCl_4$ (0.166 g, 0.439 mmol) dissolved in a mixture of 5 mL deionized H_2O and 10 mL MeOH was rapidly added to the stirring ligand solution, immediately forming a cloudy, peach suspension. After 18 h of stirring under an Ar blanket, the white solid was anaerobically filtered to yield a clear, light yellow-orange solution. The solution was reduced in volume and ether was added to precipitate a peach colored solid. The isolated solid was washed three times each with MeOH and ether and dried under an Ar flow to yield 0.161 g [Au(bme-dach)]Cl (0.356 mmol, 81.1% yield).

Counterion exchange

A solution of $NaBPh_4$ (0.122 g, 0.356 mmol) in 15 mL of MeOH was added to a yellow-orange solution of [Au(bme-dach)]Cl (0.161 g, 0.356 mmol) in 25 mL of MeOH, and allowed to stir at 22 °C for 16 h. The resulting reaction mixture was anaerobically filtered to separate the peach solid from the clear, colorless solution. The solid was redissolved in MeCN, filtered to remove residual NaCl, and ether added to precipitate solid product, [Au(bme-dach)]BPh$_4$. The solid was washed three times each with MeOH and ether before drying *in vacuo* to yield 0.122 g (0.166 mmol, 37.8% yield). X-ray quality crystals were obtained by slow evaporation from a MeCN solution. ESI-Mass Spectrum in MeCN: M^+, 415; Anal. Calcd. for $C_{33}H_{38}N_2S_2Au_1$ (Mr = 723.77 g mol^{-1}): C, 54.76; H, 5.29; N, 3.87. Found: C, 55.61; H, 5.77; N, 4.15.

Apparatus and procedures

Electrospray Ionisation Time of Flight Mass Spectrometry, ESI-TOFMS. Mass spectra were acquired on a Waters-Micromass Qtof-2 for higher resolution. Electrospray conditions were maintained throughout the experiment. Samples were flowed pneumatically using a Harvard syringe pump at 5.0 μL min^{-1} with an ESI source temperature ranging from 90–120 °C to provide efficient dissolution. Capillary voltage was operated in positive ionization mode at 2.8 kV and a cone voltage of 40 V was used throughout the experiment. The ESI-MS data for the reaction between the complexes [PtCl(dien)]Cl and [Zn(bme-dach)]$_2$ were collected using the ThermoFinnigan LCQ electrospray ion-trap (LCQ-MS) in positive mode. Acquired spectra were compared to the predicted isotope distribution patterns for each of the compounds calculated using IsoPro 3.0 Program.[26]

Solutions employed in ESI-TOFMS. The conditions followed those previously described.[16] Stock solutions of palladium and gold compounds (10^{-3} mol L^{-1}) were made up by dissolving the accurately weighed amount in H_2O. The Zn chelate was dissolved in MeOH and dilution and mixing were carried out to obtain appropriate ratios of H_2O–MeOH to maintain solubility of both compounds. After mixing in an ultrasonic bath and vortex, the solution obtained was directly injected into the ESI source. Each sample was incubated at 37 °C until the next injection.

^{1}H-NMR spectroscopy. Measurements were carried out on a Varian 300 MHz NMR Spectrometer at 20 °C. Samples were prepared using D_2O 98%.

X-ray diffraction. Data for [Au(bme-dach)]BPh$_4$ and {[ZnCl(bme-dach)]$_2$Pd} were collected on a Bruker D8 GADDS general-purpose three-circle X-ray diffractometer (Cu-Kα radiation, $\lambda = 1.54178$ Å) operating at 110 K. The [Pd(bme-dach)] single crystal data were collected on a Bruker SMART 1000 CCD based diffractometer[27] (Mo-Kα radiation, $\lambda = 0.71073$ Å), also at 110 K. The structures were solved by direct methods. H atoms were added at idealized positions and refined with fixed isotropic displacement parameters equal to 1.2 times the isotropic displacement parameters of the atoms to which they were attached. Anisotropic displacement parameters were established for all non-H atoms. The following programs were employed: data collection and cell refinement for [Au(bme-dach)]BPh$_4$ and {[ZnCl(bme-dach)]$_2$Pd}, Bruker FRAMBO, CELL-NOW, and SAINT;[28-30] data collection and cell refinement for [Pd(bme-dach)], APEX-II;[28] absorption correction, SADABS;[31] structure solution and structure refinement for all structures, SHELXS-97 and SHELXL-97;[32] and molecular graphics and preparation of material for publication, SHELXTL-PLUS, version 6.14.[32] X-seed was used for the final data presentation and structure plots.[33]

Crystallographic data and the crystallographic data summaries are listed in the Supplementary Information.† Please note that the crystal used for the [Au(bme-dach)]BPh$_4$ data collection was very small (max dimension < 20 microns), resulting in weak data and high *R*-factors.

Results and discussion

Previous studies on the interaction of platinum complexes with zinc chelates employed a tandem approach of chemical synthesis and crystallographic characterization (millimolar scale) with biomolecule and mass spectral studies (micro-nanomolar scale).[15,16] The same approach was applied here and in this work we have examined the reaction pathways of Pd^{2+} and Au^{3+} compounds with [Zn(bme-dach)]$_2$ and structurally characterized the new mononuclear [Pd(bme-dach)] and [Au(bme-dach)]$^+$ and heteronuclear Pd-Zn adducts formed. ESI-MS is a powerful technique for the characterization of inorganic and organometallic complexes and it is a promising approach to identify reaction paths and compositions from which possible bonding arrangements might be inferred in solution. Care must be taken in interpreting this mass spectral data due to possible formation of new species in the gas phase under the conditions of the mass spectral acquisition. In the present case the mass spectra of the starting materials showed in all cases only one predominant peak for the molecular ion. The reactions (carried out in H_2O–MeOH mixtures) were monitored under the same conditions to minimize adventitous reactions. The major peaks corresponding to those isolated synthetically are discussed. The structures of the complexes are shown in Fig. 1.

 This journal is © The Royal Society of Chemistry 2009

Published on 17 November 2009. Downloaded by Universitat Autonoma de Barcelona on 27/10/2014 09:31:36.

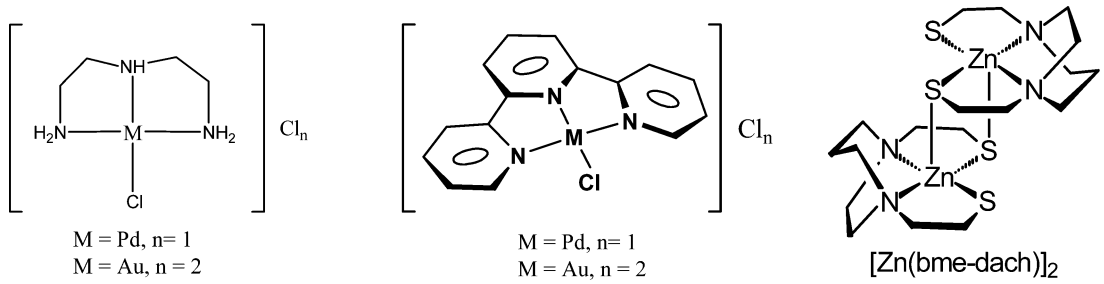

Fig. 1 Structures of the complexes $[MCl(dien)]^{n+}$, $[MCl(terpy)]^{n+}$ (M = Pd, $n = 1$; M = Au, $n = 2$) and $[Zn(bme\text{-}dach)]_2$, a small molecule model of the zinc coordination motif in zinc finger proteins.

ESI-MS studies. Reaction of $[Zn(bme\text{-}dach)]_2$ with [PdCl(terpy)]Cl

ESI-MS was used to analyze the reaction between [PdCl(terpy)]Cl and $[Zn(bme\text{-}dach)]_2$ over 22 h at different molar ratios (1 : 1 and 2 : 1, Pd : Zn). Both stoichiometries gave analogous products. Fig. 2A shows the spectrum from the 1 : 1 reaction after 1 h incubation at a concentration of ~10 μM in 90% MeOH. It is clear that multiple species are formed and even at this early time point. The peak at $m/z = 346.92$ may be assigned to the species $\{[Pd(bme\text{-}dach)]/Na^+\}^+$, which is consistent with the monoisotopic peak of the above species at $m/z = 344.88$. The isotopic distribution was consistent with the Zn–Pd exchange and the presence of a small peak at $m/z = 331.99$ corresponding to the $[ZnCl(terpy)]^+$ ion (more intense in the 2 : 1 reaction), confirmed the ligand scrambling, also observed for platinum.[16] The main heteronuclear aggregate observed at m/z 672.80 corresponded to the $\{[Zn(bme\text{-}dach)]_2Pd/H^+\}^+$ cation. Fig. 2B shows the MSMS spectrum and the fragmentation pattern of the $m/z = 672.80$ peak giving the main product ion $[Pd(bme\text{-}dach)]/Na^+\}^+$ at m/z 348.88. In addition, we observed the existence of a higher-order multinuclear aggregate such as the $\{Zn(bme\text{-}dach)_3Pd_2\}/H^+\}^+$ ion at $m/z = 996.79$. Interestingly, the MS/MS fragmentation pattern of this species was consistent with the proposed composition with loss of a [Pd(bme-dach)] moiety and the daughter peak at $m/z =$ 672.80 observed being assigned to $\{[Zn(bme\text{-}dach)]_2Pd/H^+\}^+$, Fig. 2C. The $\{[ZnCl(bme\text{-}dach)]_2Pd\}$ species is the main species formed when the compound [PdCl(terpy)]Cl reacts with the dimer $[Zn(bme\text{-}dach)]_2$, the product precipitating from solution (See Experimental Section). Crystallisation of the product confirmed the structure (see X-ray data). After 22 h, the intensity of the spectrum decreased considerably with concomitant formation of a yellow precipitate. The formation of the trinuclear species is analogous to the formation of similar heteronuclear adducts observed during the reaction of [PtCl(terpy)]Cl and [PtCl(dien)]Cl with $[Zn(bme\text{-}dach)]_2$.[16]

Reaction of $[Zn(bme\text{-}dach)]_2$ and [PdCl(dien)]Cl

We next extended our study to [PdCl(dien)]Cl, a square planar complex with a tridentate ligand coordinated to palladium, similar to [PdCl(terpy)]Cl. The intensity of the spectrum is again greatly affected by precipitation of products from solution. Fig. 3 illustrates the mass spectrum of the mixture after incubation for five minutes. Evidence for the formation of the trinuclear aggregate is seen by the presence of the peak at $m/z = 709.13$, assigned to the $\{[Zn(bme\text{-}dach)_2]PdCl\}^+$ ion. The peak at 530.20 may be assigned to $\{[Zn(bme\text{-}dach)Pd(dien)]\}^+$, corresponding to attack of the Pt(dien) electrophile on the nucleophilic zinc-bound thiolate. A similar species was identified by MS and also NMR spectroscopy in the Pt reaction.[16] Interestingly, no evidence for formation of the $[ZnCl(dien)]^+$ cation was observed. The general pathways of the Pd compounds followed those previously observed with platinum.

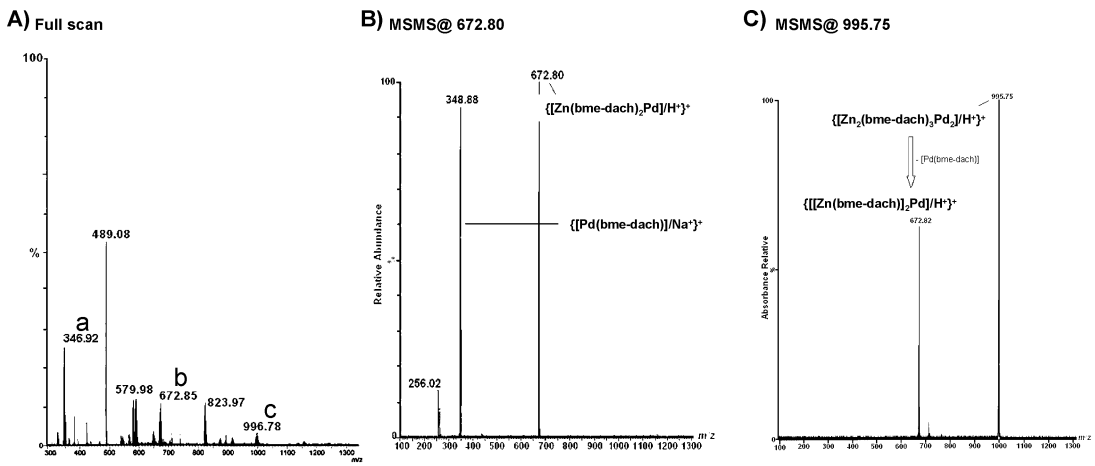

Fig. 2 (*A*) ESI-MS full scan (positive mode) of the reaction between [PdCl(terpy)]Cl and $[Zn(bme\text{-}dach)]_2$ recorded after one hour at 1 : 1 molar ratio. Species assigned: a) $\{[Pd(bme\text{-}dach)]/Na^+\}^+$, b) $\{[Zn(bme\text{-}dach)]_2Pd/H^+\}^+$ cation, and c) $\{Zn(bme\text{-}dach)_3Pd_2\}/H^+\}^+$ ion. (*B*) The MS2 of the peak 672.80 and (*C*) MS2 of the peak 995.75 from Fig. 2A. The charge outside the brackets indicates the overall charge observed in the mass spectra.

Published on 17 November 2009. Downloaded by Universitat Autonoma de Barcelona on 27/10/2014 09:31:36.

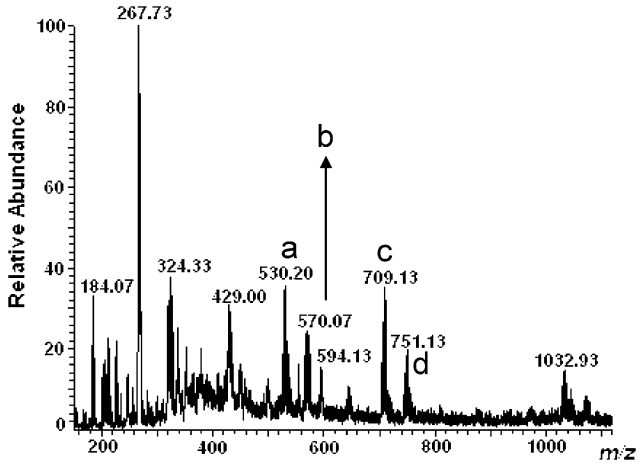

Fig. 3 The ESI-MS full scan (positive mode) of the reaction between [PdCl(dien)]Cl and $[Zn(bme\text{-}dach)]_2$ after 5 min of reaction. Species: a) $\{[Zn(bme\text{-}dach)Pd(dien)]\}^+$, b)$\{[Zn(bme\text{-}dach)]_2\}^+$, c) $\{[Zn(bme\text{-}dach)]_2PdCl\}^+$, and d) $\{[Zn(bme\text{-}dach)]_2PdCl/H_2O/Na^+\}^+$.

Reactions of gold compounds $[AuCl(dien)]Cl_2$ and $[Au(Cl(terpy)]Cl_2$ with $[Zn(bme\text{-}dach)]_2$

The reactions with the gold species (1 : 1 and 2 : 1 Au : Zn) appeared to be very fast. The spectra are remarkably simple and the profiles were very similar for both stoichiometries. The spectrum obtained immediately upon incubation of a 1 : 1 mixture of $[AuCl(dien)]^+$ and $[Zn(bme\text{-}dach)]_2$ is shown in Fig. 4. The main peak at $m/z = 437.26$ is assigned to the species with a sodium ion $\{[Au(bme\text{-}dach)]\text{-}H^+ + Na^+\}^+$ (Fig. 4, species (a)). The peak at $m/z = 873.53$ may be assigned to the heteronuclear aggregate $\{[\{Zn(bme\text{-}dach)Cl\}_2Au/Na^+/H_2O]\}$ respectively (Fig. 4, species (c)). In the 2 : 1 incubation of $[AuCl(dien)]Cl_2$ and $[Zn(bme\text{-}dach)]_2$, a companion peak at $m/z = 849.09$ is attributed to loss of the Na^+ ion, $\{[\{Zn(bme\text{-}dach)Cl\}_2Au/H_2O]\}^+$, Figure S3.† An interesting peak seen for both 1 : 1 and 2 : 1 incubations with $[AuCl(dien)]^+$ is that of $m/z = 655.40$ (Fig. 4, species (b)), corresponding to $\{[Au(bme\text{-}dach)_2]/Na^+/\text{-}H^+\}$. This may suggest some form of a gold dimer as a precursor and the species may also contain disulfide bonds. In this respect it is noteworthy, as stated, that evidence has been presented for Au^{3+} reduction followed by release of the bound ligand and eventual coordination of a Au^{1+} ion to a protein side chain when Au^{3+} anticancer compounds are allowed to react with ubiquitin and cytochrome c.[13] Further studies are underway to confirm this suggestion. For $[AuCl(terpy)]^+$, the spectrum taken immediately after the 1 : 1 incubation yielded a peak at $m/z = 415.09$ which was assigned to the metal exchanged ion $\{[Au(bme\text{-}dach)\}^+$, Figure S4.† The main heteronuclear aggregate is a small peak at $m/z = 763.09$ corresponding to $\{[Zn(bme\text{-}dach)]_2Au\}^+$, which after 40 h is the main species observed.

Structural characterization of Pd^{2+} and Au^{3+} substituted chelates

In general, the reactivity profile for the Pd^{2+} and Au^{3+} compounds follows that of platinum. Incorporation of M into the bme-dach chelate with liberation of Zn^{2+} is seen. It is also of interest that the heterotrinuclear dithiolate-bridged Zn,M,Zn species appears to be the predominant multinuclear aggregate in all cases. As expected, the reactions appeared to be faster for the Pd^{2+} and Au^{3+} species. To confirm the structural assignments the principal products were synthesized on a macro scale, in contrast to the nano scale of the MS experiments.

Synthesis and X-ray results for the $\{[Zn(bme\text{-}dach)Cl]_2Pd\}$ complex

In order to isolate and quantify this compound, the same reaction as described above was carried out on a larger scale. The yellow product was characterized as the heteronuclear $[ZnCl(bme\text{-}dach)]_2Pd]$ complex, confirmed by elemental analysis and X-ray diffraction analysis of a single crystal. Cell parameters and data collection summaries for $\{[ZnCl(bme\text{-}dach)]_2Pd\}$, $[Pd(bme\text{-}dach)]$ and $[Au(bme\text{-}dach)]BPh_4]$ are given in Table 1, with selected metric parameters listed in Table 2.

The molecular structure shown in Fig. 5 illustrates the Zn_2Pd trimetallic stair-step product resulting from the 2Pd:1Zn reaction. The ball and stick X-ray crystal structure of $\{[ZnCl(bme\text{-}dach)]_2Pd\}$ shows the zinc coordinated to two sulfurs, two nitrogens and an apical chloride in a penta-coordinate geometry. The N_2S_2 atoms (without Zn) form a plane with a mean deviation of 0.0120 Å. In contrast to the $\{[ZnCl(bme\text{-}dach)]_2Pt\}$structure, which contains some asymmetry, the $\{[ZnCl(bme\text{-}dach)]_2Pd\}$ complex is symmetric with half of its molecule as a symmetry generated duplicate of the other half. The hinge angles, as defined above, are larger for the Pt^{2+} derivative as well as asymmetrical, 104.5° and 99.0°.

The molecular structure of the isolated product confirms the reactivity of the Zn-bound thiolates to form stable bridges to Pd^{2+}, while retaining the Zn–S bond. This Zn-(μ-SR)$_2$-Pd^{2+} complex is relevant to possible interactions between heavy metal compounds and Zinc fingers from NCp7.

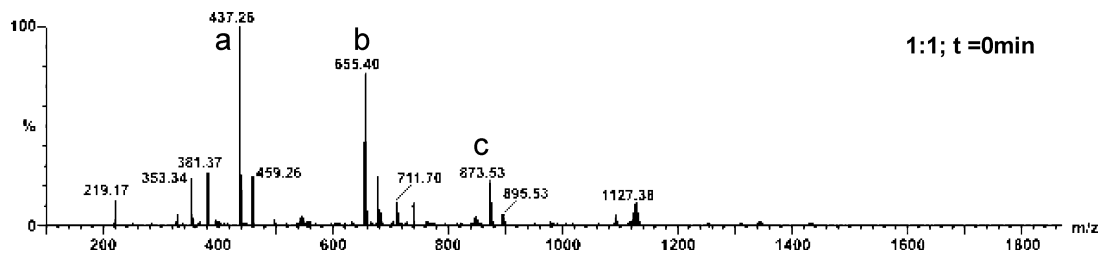

Fig. 4 The ESI-MS full scan (positive mode) of the reaction between $[AuCl(dien)]Cl_2$ and $[Zn(bme\text{-}dach)]_2$ immediately upon incubation. Species: a) $\{[Au(bme\text{-}dach)]\text{-}H^+ + Na^+\}^+$, b) $\{[Au(bme\text{-}dach)_2]/Na^+/\text{-}H^+\}$, and c) $\{[\{Zn(bme\text{-}dach)Cl\}_2Au/Na^+/H_2O]\}$.

 This journal is © The Royal Society of Chemistry 2009

Published on 17 November 2009. Downloaded by Universitat Autonoma de Barcelona on 27/10/2014 09:31:36.

Table 1 Crystal data for {[ZnCl(bme-dach)]$_2$Pd}, [Pd(bme-dach)] and [Au(bme-dach)][BPh$_4$]

	{[ZnCl(bme-dach)]$_2$Pd}	[Pd(bme-dach)]	[Au(bme-dach)]BPh$_4$
Empirical formula	$C_{9.5}H_{18.5}Cl_{12.5}N_2S_2Pd_{0.5}Zn$	$C_9H_{18}N_2S_2Pd$	$C_{33}H_{38}BN_2S_2Au$
Formula weight	432.08	324.77	734.55
T/K	110(2)	110(2)	110(2)
Wavelength/Å	1.54178	0.71073	1.54178
Crystal system	Monoclinic	Orthorhombic	Monoclinic
Space group	$P2_1/c$	*Pnma*	$P2_1/c$
Unit cell dimensions	$a = 7.4293(2)$ Å; $\alpha = 90°$ $b = 12.400(8)$ Å; $\beta = 97.128(2)°$ $c = 16.645(3)$ Å; $\gamma = 90°$	$a = 9.961(5)$ Å; $\alpha = 90°$ $b = 15.105(7)$ Å; $\beta = 90°$ $c = 7.514(4)$ Å; $\gamma = 90°$	$a = 10.643(4)$ Å; $\alpha = 90°$ $b = 14.184(5)$ Å; $\beta = 117.051(18)°$ $c = 21.407(7)$ Å; $\gamma = 90°$
Z	4	4	4
Absorption coefficient/mm^{-1}	13.312	1.974	11. 149
Volume/Å^3	1521.66(8)	1130.5(9)	2878.1(18)
Goodness-of-fit on F^2	1.040	1.098	1.062
Final R indices [$I > 2\sigma(I)$]	$R_1 = 0.0295$, w$R_2 = 0.0769$	$R_1 = 0.0618$, w$R_2 = 0.1614$	$R_1 = 0.0948$, w$R_2 = 0.2289$
R indices (all data)	$R_1 = 0.0349$, w$R_2 = 0.0769$	$R_1 = 0.0905$, w$R_2 = 0.1809$	$R_1 = 0.1704$, w$R_2 = 0.2721$

Table 2 Selected bond lengths (Å) for {[ZnCl(bme-dach)]$_2$Pd}, [Pd(bme-dach)] and [Au(bme-dach)] complexes

{[ZnCl(bme-dach)]$_2$Pd}		[Pd(bme-dach)]		[Au(bme-dach)]$^+$	
Pd(1)-S(1)	2.3510(8)	Pd(1)-S(1)	2.2825(2)	Au(1)-S(1)	2.290(6)
Pd(1)-S(2)	2.3543(8)			Au(1)-S(2)	2.293(6)
Zn(1)-S(1)	2.4373(9)	Pd(1)-N(1)	2.074(7)	Au(1)-N(1)	2.18(2)
Zn(1)-S(2)	2.4219(9)			Au(1)-N(2)	2.12(2)
Zn(1)-N(1)	2.157(2)	—		—	
Zn(1)-N(2)	2.185(2)	—		—	
Zn(1)-Cl(1)	2.2415(9)	—		—	

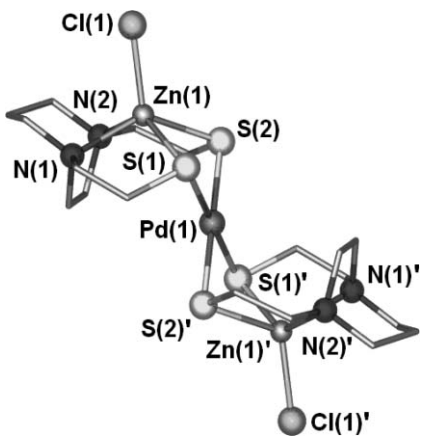

Fig. 5 Molecular structure of {[ZnCl(bme-dach)]$_2$Pd}. The second half of the molecule is generated by inversion through palladium.

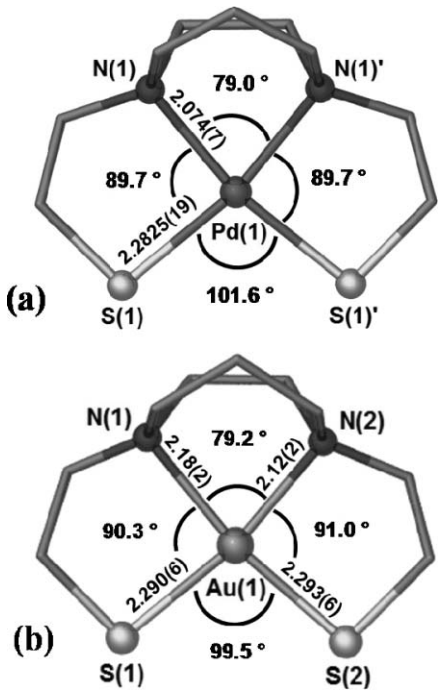

Fig. 6 (a) Ball and stick illustration of [Pd(bme-dach)] in a bird's eye view of the molecule. (b) Ball and stick representation of [Au(bme-dach)]$^+$ with the BPh$_4^-$ counterion omitted for clarity.

Molecular structures of [Pd(bme-dach)] and [Au(bme-dach)]BPh$_4$

The larger scale direct syntheses of [Pd(bme-dach)] and [Au(bme-dach)]BPh$_4$ were executed to support the Zn/Pd and Zn/Au metal exchange within the aforementioned ESI-MS monitored reactions and MS/MS fragmentations. Table 1 includes the crystallographic data for both complexes. Fig. 6 displays the ball and stick representations of the [Pd(bme-dach)] and [Au(bme-dach)]$^+$ molecular structures, with selected bond distances and angles denoted within the figure.

Both complexes are highly regular square planes and contain similar metric parameters to those of the Pt(bme-dach) derivative.[16] Reminiscent of the Pt^{2+} analogue, the [Pd(bme-dach)] is comprised of a perfect N_2S_2 plane, where one half of the molecule is the symmetry-generated product of the other. Furthermore, the Pd^{2+} is displaced from the N_2S_2 best plane by 0.0176 Å, whereas the Pt^{2+} resides within the same ligand set with a lesser deviation (0.0003 Å). The crystal packing of the Pd(bme-dach) molecule

Published on 17 November 2009. Downloaded by Universitat Autonoma de Barcelona on 27/10/2014 09:31:36.

Table 3 Comparison of selected bond angles and distances within [M(bme-dach)] structures, where M = Ni^{2+},[19] Pd^{2+}, Pt^{2+},[16] and Au^{3+}

[M(bme-dach)], M =	Ni^{2+}	Pd^{2+}	Pt^{2+}	$[Au^{3+}]^{+}$
M–N (Å)	1.940(4)	2.074(7)	2.089(1)	2.18(2), 2.12(2)
M–S (Å)	2.164(1)	2.283(2)	2.298(3)	2.290(6), 2.293(6)
∠ N–M–N (°)	82.5(2)	79.0(4)	80.6(8)	79.2(8)
∠ S–M–S (°)	95.4(1)	101.7(1)	102.4(2)	99.5(2)
M displacement from N_2S_2 plane (Å)	n/a	0.0176	0.0003	0.0016

displays disorder of the C(2) atom within the pendant thiolate arm (see Figure S5†). Note that disorder of only the prominent (elbow) carbon was modelled in the structure refinement. The ripple effect of this disorder causing disorder in C(3) and C(5) and other associated carbon atoms was not modelled.

The $[Au(bme\text{-}dach)]^{+}$ structure contains an N(1)N(2)S(1)S(2) plane with a mean deviation of 0.0228 Å, and the Au^{3+} shifted only 0.0016 Å outside of this plane. As previously mentioned, the bond distances and angles closely parallel those found within the [Pt(bme-dach)], displayed in Table 3 along with comparisons to the Ni^{2+} analogue.[16,19]

As revealed in Table 3 above, the development of the Pd^{2+} and Au^{3+} derivatives adds to the library of existing M(bme-dach) compounds. The Zn/Au metal exchange reported in the present work rendered the first indication of possible formation of an Au^{3+} derivative to exist in this bme-dach collection. As expected, the M–N and M–S bond distances lengthen as the central metal ion descends from a first to second to third row transition metal. In terms of the ∠ N–M–N and ∠ S–M–S, both the size of the central metal ion and the flexibility of the ligand play a role in the angles ultimately observed. With regard to the metal ion, as the size increases, the ∠ S–M–S normally increases within this tetradentate ligand set. Such an "opening" of the ∠ S–M–S is associated with a concomitant "pinching" or decrease in the ∠ N–M–N. This trend is observed between the Ni^{2+}, Pd^{2+}, and Pt^{2+} complexes. The Au^{3+} complex, however, does not continue to show an increase in ∠ S–M–S with a corresponding decrease in ∠ N–M–N. Although it is a third row transition metal, the higher oxidation state and thus decrease in ionic radii may contribute to its detected angles being more comparable to those found within the Pd^{2+} complex.

Conclusions

The reactions of isostructural Pd^{2+} and Au^{3+} compounds with $[Zn(bme\text{-}dach)]_2$ showed similar behavior to that of previously studied Pt.[16] Zinc preservation of cysteine thiolate nucleophilicity renders the sulfur sufficiently reactive towards electrophilic platinum moieties to yield Zn-(μ-SR)-Pt bridged, multi-metallic, and metal-exchanged species. In the case of Pt^{2+}, intermediate species containing the Pt(dien) moiety could be identified by both NMR and crystallographic methods. The Zn-(μ-SR)-Pt-bridged species, [(ZnCl(bme-dach))(Pt(dien))]Cl, is, to our knowledge, the first structurally isolated Zn–Pt bimetallic thiolate-bridged model demonstrating the interaction between Zn-bound thiolates and Pt^{2+}. Most recently, the -$W(CO)_4$ residue has also been shown to form dinuclear dithiolate-bridged species with the advantage that IR spectral reporting *via* ν(CO) stretching frequencies is possible.[34] In the present study, the faster reactions on Pd^{2+} only allowed limited mass spectrometric evidence for analogous Pd(dien) species, while for Au^{3+}, only species corresponding to complete ligand displacement (dien, terpy) were seen even at the earliest time points. As stated, the development of the Pd^{2+} and Au^{3+} derivatives adds to the library of existing M(bme-dach) compounds (Table 3). Further, the exploration of the interactions of $[Zn(bme\text{-}dach)]_2$ with Pt^{2+}, Pd^{2+}, and Au^{3+} complexes has amply demonstrated the capability of such species to form stable thiolate-bridged heteronuclear aggregates. Indeed, the thermodynamic "sink" appears to be the trinuclear dithiolate-bridged {Zn,M,Zn} aggregate. Interestingly, analogous $[Ni(N_2S_2)]_2M^{2+}$ (M = Ni, Pd, Pt) have also been reported.[35,36]

One reason for this investigation has been to use the chemistry of model zinc chelates as predictors of structure and reactivity on zinc fingers. Metal ion replacement reactions of zinc in zinc finger proteins are well documented and may have important biological implications. Replacement of Zn by metal ions such as Pb^{2+} and Ni^{2+} may contribute to their "toxic" effects.[37,7] Modification of the zinc finger Zn–S sites, through alkylation, oxidation, or metalation, may disrupt zinc protein conformation, thus altering and/or inhibiting their critical biological functions.[8,38] An analogous study has investigated the reactions of the [MCl(chelate)] compounds of this study (M = Pt^{2+}, Pd^{2+} or Au^{2+} and chelate = diethylenetriamine, dien or 2,2′,2″-terpyridine, terpy) with the C-terminal finger of the HIV nucleocapsid NCp7 zinc finger.[39] In the case of [M(dien)] species, Pt^{2+} and Pd^{2+} behaved in a similar fashion with evidence of adducts caused by displacement of Pt–Cl or Pd–Cl by zinc-bound thiolate. Labilization, presumably under the influence of the strong *trans* influence of thiolate, resulted in loss of ligand (dien) as well as zinc ejection and formation of species with only Pd^{2+} or Pt^{2+} bound to the finger. For both Au^{3+} compounds the reactions were very fast and only "gold fingers" with no ancillary ligands were observed.[39] For all terpyridine compounds, ligand scrambling and metal exchange occurred with formation of $[Zn(terpy)]^{2+}$. Thus, as with the platinum case,[15] the chemistry and structures described in this paper also represent viable descriptions for the reactions of metal complexes with zinc fingers. In the present case, the isolation and characterization of an Au^{3+} chelate suggests that Au^{3+}, as well as Au^{1+} could be incorporated into a zinc protein site – further studies will address this question.

Acknowledgements

The authors gratefully acknowledge the financial support of The National Science Foundation (CHE-0616695/CHE-0910679 to MYD and CHE-0616768 to NPF). Q.A.P. and N.P.F. acknowledge contributions from Conselho Nacional de Pesquisa e Desenvolvimento (CNPq-210265/2006-0) for supporting the International Postdoctoral Fellowship of Dr. Queite A. de Paula. MYD also

 This journal is © The Royal Society of Chemistry 2009

acknowledges contributions from the R. A. Welch Foundation (A-0924).

Published on 17 November 2009. Downloaded by Universitat Autonoma de Barcelona on 27/10/2014 09:31:36.

References

1 W. Maret and Y. Li, *Chem. Rev.*, 2009, **109**, 4682–4707.
2 J. M. N. Hoovers, M. Mannens, R. John, J. Bliek, V. van Heyningen, D. J. Porteous, N. J. Leschot, A. Westerveld and P. F. R. Little, *Genomics*, 1992, **12**, 254.
3 K. Sakaguchi, N. Zambrano, E. T. Baldwin, B. A. Shapiro, J. W. Erickson, J. G. Omichinski, G. M. Clore, A. M. Gronenborn and E. Appella, *Proc. Natl. Acad. Sci. U. S. A.*, 1993, **90**, 5219.
4 J. W. Bess Jr., P. J. Powell, H. J. Issaq, L. J. Schumack, M. K. Grimes, L. E. Henderson and L. O. Arthur, *J. Virol.*, 1992, **66**, 840.
5 J. L. Larabee, J. R. Hocker and J. S. Hanas, *Chem. Res. Toxicol.*, 2005, **18**, 1943.
6 J. M. Berg and H. A. Godwin, *Annu. Rev. Biophys. Biomol. Struct.*, 1997, **26**, 357.
7 A. Witkiewicz-Kucharczyk and W. Bal, *Toxicol. Lett.*, 2006, **162**, 29.
8 A. I. Anzellotti, Q. Liu, M. J. Bloemink, J. N. Scarsdale and N. Farrell, *Chem. Biol.*, 2006, **13**, 539.
9 D. A. Sartori, B. Miller, U. Bierbach and N. Farrell, *JBIC, J. Biol. Inorg. Chem.*, 2000, **5**, 575.
10 Y. Zou, B. Van Houten and N. Farrell, *Biochemistry*, 1993, **32**, 9632.
11 M. L. Handel, A. de Fazio, C. W. Watts, R. O. Day and R. L. Sutherland, *Mol. Pharmacol.*, 1991, **40**, 613.
12 W. Kaim and B. Schwederski, in *Bioinorganic Chemistry: Inorganic Elements in the Chemistry of Life*, G. Meyer and A. Nakamura, Eds., Wiley, New York, 1994, pp. 374-375.
13 A. Casini, C. Hartinger, C. Gabbiani, E. Mini, P. J. Dyson, B. K. Keppler and L. Messori, *J. Inorg. Biochem.*, 2008, **102**, 564.
14 C. Demicheli, F. Frezard, J. B. Mangrum and N. P. Farrell, *Chem. Commun.*, 2008, 4828.
15 Q. Liu, M. Golden, M. Y. Darensbourg and N. Farrell, *Chem. Commun.*, 2005, 4360.
16 E. Almaraz, Q. A. de Paula, Q. Liu, J. H. Reibenspies, M. Y. Darensbourg and N. Farrell, *J. Am. Chem. Soc.*, 2008, **130**, 6272.
17 C. A. Grapperhaus, T. Tuntulani, J. H. Reibenspies and M. Y. Darensbourg, M., *Inorg. Chem.*, 1998, **37**, 4052.
18 C. A. Grapperhaus, M. J. Maguire, T. Tuntulani and M. Y. Darensbourg, *Inorg. Chem.*, 1997, **36**, 1860.
19 J. J. Smee, M. L. Miller, C. A. Grapperhaus, J. H. Reibenspies and M. Y. Darensbourg, *Inorg. Chem.*, 2001, **40**, 3601.
20 F. Basolo, H. B. Gray and R. G. Pearson, *J. Am. Chem. Soc.*, 1960, **82**, 4200.
21 S. D. Cummings, *Coord. Chem. Rev.*, 2009, **253**, 449.
22 T. Tuntulani, G. Musie, J. H. Reibenspies and M. Y. Darensbourg, *Inorg. Chem.*, 1995, **34**, 6279.
23 M. Y. Darensbourg, T. Tuntulani and J. H. Reibenspies, *Inorg. Chem.*, 1995, **34**, 6287.
24 S. Morgan and F. H. Burstall, *J. Chem. Soc.*, 1937, 1649.
25 L. S. Hollis and S. J. Lippard, *J. Am. Chem. Soc.*, 1983, **105**, 4293.
26 Isopro3.1 Program.
27 *SMART 1000 CCD*, Bruker Analytical X-ray Systems, Madison, WI, 1999.
28 Bruker-Nonius Inc., *FRAMBO*, Version 4.1.13, Madison, Wisconsin, USA, 2003.
29 G. Sheldrick, *CELL-NOW*, University of Göttingen, Germany, 2003.
30 Bruker-Nonius Inc., *SAINT*, Madison, Wisconsin, USA, 2003.
31 Bruker-Nonius, *APEX II. Version*, 2008.6-0. Bruker-Nonius Inc., Madison, Wisconsin, USA, 2008.
32 G. Sheldrick, *Acta Cryst.*, 2008, *A64*, 112-122, and related references therein.
33 L. J. Barbour, *J. Supramol. Chem.*, 2001, **1**, 189.
34 E. Almaraz, W. S. Foley, J. A. Denny, J. H. Reibenspies, M. L. Golden and M. Y. Darensbourg, *Inorg. Chem.*, 2009, **48**, 5288.
35 M. V. Rampersad, S. P. Jeffery, J. H. Reibenspies, C. G. Ortiz, D. J. Darensbourg and M. Y. Darensbourg, *Angew. Chem., Int. Ed.*, 2005, **44**, 1217.
36 M. L. Golden, C. M. Whaley, M. V. Rampersad, J. H. Reibenspies, R. D. Hancock and M. Y. Darensbourg, *Inorg. Chem.*, 2005, **44**, 875.
37 J. C. Payne, M. A. ter Horst and H. A. Godwin, *J. Am. Chem. Soc.*, 1999, **121**, 6850.
38 J. S. Hanas, J. L. Larabee and J. R. Hocker, in *Zinc Finger Proteins: From Atomic Contact to Cellular Function*, S. Iuchi and N. Kuldell, Eds., Landes Bioscience, Austin, TX, 2005, pp. 39-46.
39 Q. A. de Paula, J. B. Mangrum and N. P. Farrell, *J. Inorg. Biochem.*, 2009, **103**, 1347.